ELSEVIER

Journal of Molecular Structure 602-603 (2002) 257–267

Journal of
MOLECULAR
STRUCTURE

www.elsevier.com/locate/molstruc

Towards understanding the origins of the different specificities of binding the reduced (NADPH) and oxidised ($NADP^+$) forms of nicotinamide adenine dinucleotide phosphate coenzyme to dihydrofolate reductase ☆

Vladimir I. Polshakov[a,b], Rodolfo R. Biekofsky[a], Berry Birdsall[a], James Feeney[a,*]

[a]*Division of Molecular Structure, National Institute for Medical Research, The Ridgeway, Mill Hill, London NW7 1AA, UK*
[b]*Center for Drug Chemistry, Moscow 119815, Russian Federation*

Received 2 March 2001; accepted 18 March 2001

Abstract

Lactobacillus casei dihydrofolate reductase (DHFR) binds more than a thousand times tighter to NADPH than to $NADP^+$. The origins of the difference in binding affinity to DHFR between NADPH and $NADP^+$ are investigated in the present study using experimental NMR data and hybrid density functional, B3LYP, calculations. Certain protein residues (Ala 6, Gln 7, Ile 13 and Gly 14) that are directly involved in hydrogen bonding with the nicotinamide carboxamide group show consistent differences in ^1H and ^{15}N chemical shift between NADPH and $NADP^+$ in a variety of ternary complexes. B3LYP calculations in model systems of protein-coenzyme interactions show differences in the H-bond geometry and differences in charge distribution between the oxidised and reduced forms of the nicotinamide ring. GIAO isotropic nuclear shieldings calculated for nuclei in these systems reproduce the experimentally observed trends in magnitudes and signs of the chemical shifts. The experimentally observed reduction in binding of $NADP^+$ compared with NADPH results partly from $NADP^+$ having to change its nicotinamide amide group from a *cis*- to a *trans*-conformation on binding and partly from the oxidised nicotinamide ring of $NADP^+$ being unable to take up its optimal hydrogen bonding geometry in its interactions with protein residues.

Keywords: *Lactobacillus casei* dihydrofolate reductase; Nicotinamide adenine dinucleotide phosphate; Nuclear magnetic resonance; Density functional theory; Chemical shift; Hydrogen bond

1. Introduction

Dihydrofolate reductase (EC 1.5.1.3) catalyses the reduction of 7,8-dihydrofolate to 5,6,7,8-tetrahydrofolate using nicotinamide adenine dinucleotide phosphate (NADPH) as the coenzyme. Tetrahydrofolate is an important intermediate in the subsequent biosynthesis of purines, dTMP, serine and methionine [1], and high intracellular concentrations of tetrahydrofolate need to be maintained particularly for

☆ Dedicated to Professor Graham A. Webb on the occasion of his 65th birthday.

* Corresponding author. Tel.: +44-208-959-3666; fax: +44-208-906-4477.

E-mail address: JFeeney@nimr.mrc.ac.uk (J. Feeney).

Abbreviations: B3LYP, Becke's Three Parameter Hybrid Functional using the Lee, Yang and Parr Correlation Functional; DFT, Density Functional Theory; DHFR, dihydrofolate reductase; GIAO, Gauge-Independent Atomic Orbital; HSQC, heteronuclear single-quantum correlation spectroscopy; LCS, Ligand-induced chemical shift; $NADP^+$, oxidised nicotinamide adenine dinucleotide phosphate; NADPH, reduced nicotinamide adenine dinucleotide phosphate; NMR, nuclear magnetic resonance

0022-2860/02/$ - see front matter
PII: S0022-2860(01)00687-1

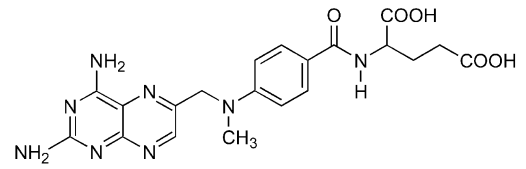

1

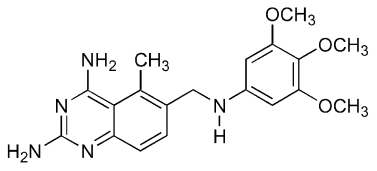

2

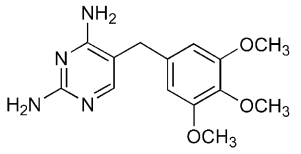

3

Scheme 1.

the DNA replication process preceding cell division. Dihydrofolate reductase is thus an essential enzyme in the cell and is the target for antifolate drugs that act by inhibiting the enzyme in malignant or parasitic cells. Inhibitors of dihydrofolate reductase have been used in the treatment of bacterial, protozoal and fungal infections and various neoplastic diseases. These drugs include methotrexate **1** (antineoplastic), trimetrexate **2** (antineoplastic and antibacterial), trimethoprim **3** (antibacterial) and pyrimethamine (antiprotozoal) shown in Scheme 1 (structures **1**–**3** (methotrexate, trimetrexate and trimethoprim)).

During the enzymatic reduction of 7,8-dihydrofolate, a hydride ion from the C4-position of the reduced nicotinamide ring of NADPH **4** is transferred to position 6 of the 7,8-dihydrofolate molecule and results in the coenzyme $NADP^+$ **5** having an oxidised nicotinamide ring. The reduced nicotinamide ring of NADPH is neutral and non-aromatic, and is slightly puckered into a boat non-planar conformation [2]. Upon oxidation, the nicotinamide ring becomes positively charged and aromatic. Coenzyme binding to DHFR is extremely sensitive to the change in oxidation state of the nicotinamide ring. For example, DHFR binds to NADPH more than a thousand times more tightly than it does to $NADP^+$ [3,4]. The large difference in affinity for DHFR shown by the reduced and oxidised forms of the coenzyme is consistent with a mechanism by which the enzyme can easily eliminate the oxidised form ($NADP^+$) and thus allow the binding of a new molecule of NADPH to provide an active DHFR-coenzyme-substrate complex [5,6]. Nicotinamide coenzyme-dependent dehydrogenases continue to attract great interest because of their importance in biological systems and their fascinating substrate selectivity and stereoselectivity [2,7–14].

X-ray [15] and NMR [16] determined structures of DHFR complexes containing NADPH or $NADP^+$ reveal that the overall structure of the nicotinamide binding pocket does not vary very much between the reduced and oxidised states of the coenzyme. However, from the observed large difference in binding affinity between the reduced and oxidised forms of the coenzyme to DHFR it seems logical to assume that there are more attractive interactions between the enzyme and the reduced form of the coenzyme than between the enzyme and the oxidised form. It has been observed that the binding pocket for the nicotinamide moiety contains no formally charged side-chains that could interact with the positive charge of the oxidised nicotinamide ring, nor are there any aromatic side-chains to provide stacking interactions with the aromatic oxidised nicotinamide of $NADP^+$ [17]. Earlier NMR studies indicated that there are large chemical shift differences between corresponding protein side-chain signals in complexes of *Lactobacillus casei* DHFR with NADPH and $NADP^+$ [18]. These differences reflect changes arising from the different interactions between nicotinamide pocket residues of the protein and the reduced or oxidised form of the coenzyme. The shielding of a nucleus is a very sensitive probe of its electronic environment and NMR chemical shift differences can report information related to changes in individual atoms that cannot be obtained otherwise.

The present study is aimed at using experimental ^1H and ^{15}N chemical shift data from protein nuclei in the environment of the nicotinamide moiety to gain further insights into the binding and structural differences between complexes of DHFR formed with

NADPH and $NADP^+$. Several complexes of ^{15}N-labelled *L. casei* DHFR with reduced and oxidised forms of the coenzyme have been examined in order to observe the effects that the change in coenzyme structure has on the ^1H and ^{15}N chemical shifts of the enzyme. Consistent differences in ^1H and ^{15}N chemical shift of certain residues were found between NADPH and $NADP^+$ in a variety of ternary complexes. In order to rationalise the observed experimental results, DFT calculations in model systems of protein-coenzyme interactions were performed and GIAO calculations of the isotropic ^1H and ^{15}N nuclear shieldings for these nuclei were carried out. The results of such calculations may help towards unravelling the mechanism of action of this enzymatic complex at the molecular level. The characterisation of the network of interactions involved in binding the oxidised and reduced nicotinamide rings to DHFR in the two complexes could contribute to a better understanding of how the enzyme 'recognises' the local structural differences in the coenzyme and how these translate into differences in macroscopic binding constants.

2. Materials and methods

2.1. Materials

^{15}N-labelled *L. casei* dihydrofolate reductase was prepared as described previously from an *Escherichia coli* strain in which the structural gene for the *L. casei* enzyme had been cloned [19,20]. Methotrexate, trimethoprim, trimetrexate, $NADP^+$ and NADPH were all obtained from Sigma. The enzyme complexes were prepared by dialysing the enzyme in the presence of the appropriate ligand before freeze-drying and redissolving to give the required concentrations. The chemical shifts of marker signals used for monitoring the presence of oxidised or reduced coenzyme were described previously [18].

2.2. NMR experiments

The NMR experiments were carried out on Varian Unity, Unity Plus and INOVA spectrometers operating at proton frequencies of 500, 600 and 600 MHz, respectively. All the NMR experiments used the Watergate technique for water suppression [21] and the GARP sequence [22] for ^{15}N decoupling during the detection period. Quadrature detection in all indirectly detected dimensions was achieved using the method of States and coworkers [23]. The two-dimensional $^1H/^{15}N$ HSQC sequence used in the experiments was essentially the same as that proposed by Mori and coworkers [24]. The experiments were performed using the parameters reported previously [25]. Signal assignments were made using two-dimensional and three-dimensional $^1H/^{15}N$ experiments as described previously for TMQ [26] and for MTX [27].

2.3. Quantum mechanical calculations

Systems 1 and 2 were extracted from the NMR solution structure of the ternary complex DHFR–NADPH–TMP [16] and used for further geometry optimisation. All electronic structure calculations were carried out with the GAUSSIAN 98 suite of programs [28]. Geometry optimisation calculations on model System 1 (see Fig. 3) were carried out with the Hartree–Foch method using the 3-21G basis set [29–31] whereas those on model System 2 (see Fig. 4) were carried out with the Density Functional Theory (DFT) [32] method using the 6.311G(3d,2p) basis set [33,34]. The second set of calculations used Becke's hybrid exchange functional [35] and the nonlocal correlation functional of Lee, Yang and Parr (B3LYP) [36]. All the geometry optimisations in Systems 1 and 2 were performed without symmetry constraints using the Berny algorithm [37] available as a default in GAUSSIAN 98 [28].

The ^1H and ^{15}N chemical shieldings were calculated using the GIAO method [38] with a 6.311++G(2d,p) basis set [33,34]. In order to calculate absolute values of chemical shifts, isotropic shieldings were calculated for TMS and NH_3 using the same basis set. A value of 18 ppm (chemical shift difference between NH_3 in gas and liquid phases, [39]) was subtracted from the values of the calculated ^{15}N chemical shifts.

3. Results and discussion

3.1. Structure of the nicotinamide-binding pocket in DHFR complexes

A detailed analysis of the available three-dimensional structures of DHFR complexes with reduced

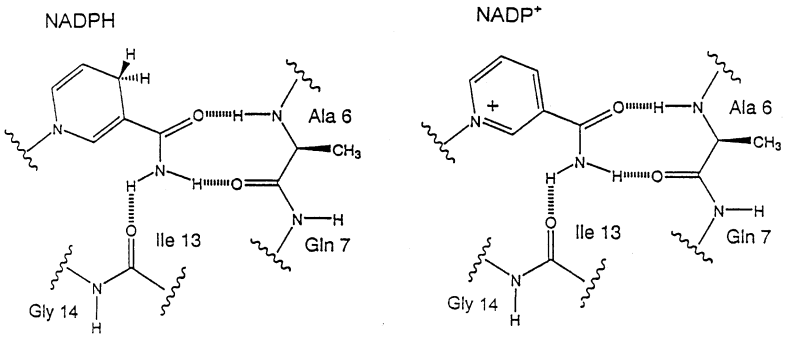

Fig. 1. Schematic drawing of hydrogen bond network between *L. casei* DHFR residues and the nicotinamide carboxamide group of NADPH and $NADP^+$.

and oxidised forms of the coenzyme showed that no large structural changes in the protein accompanies the change in oxidation state of the nicotinamide ring (Ref. [15] and data from Brookhaven Protein Data Bank]. The overall orientation of the nicotinamide rings in the binding site and the protein residues involved in the nicotinamide ring interactions are the same in the different complexes. Thus, the same characteristic pattern of hydrogen bonds is found between the coenzyme amide group atoms and the same protein backbone atoms of residues Ala 6 and Ile 13 (see Fig. 1). For example, the oxygen atom of the coenzyme amide group forms a hydrogen bond with the backbone HN group of Ala 6, and the coenzyme NH_2 protons form hydrogen bonds with the carbonyl oxygen atoms of residues Ala 6 and Ile 13 in complexes with both NADPH and $NADP^+$ (Fig. 1). This pattern of hydrogen bonds was also found in the NMR solution structure of the ternary complex of *L. casei* DHFR with TMP and NADPH [16]. The positions of the interacting protein residues in the overall structure are shown in Fig. 2.

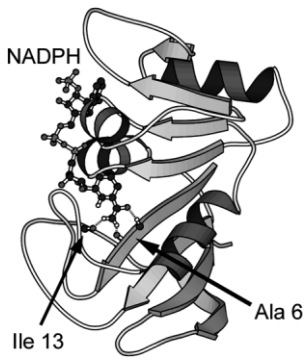

Fig. 2. Structure showing NADPH bound to *L. casei* DHFR (taken from the structure of the ternary complex DHFR–NADPH–TMP [16]. The hydrogen bond interactions between the nicotinamide carboxamide group and the protein backbone are shown with dotted lines.

3.2. DHFR ^1H and ^{15}N NMR signals in $NADP^+$ and NADPH complexes

NMR spectra for several binary and ternary complexes of [^{15}N]-DHFR were recorded and analysed. These included the binary complexes of the enzyme with TMP, MTX and TMQ, and ternary complexes with TMP, MTX and TMQ, each together with either NADPH or $NADP^+$. All the complexes exist as single conformations except for the DHFR–TMP–$NADP^+$ complex which has two conformations in a ~1:1 ratio [40–42]. The resonances arising from each complex were assigned to the residues in the DHFR sequence according to standard procedures described previously [26,27,43]. In the case of the DHFR–TMP–$NADP^+$ complex, the two interconverting conformers have been characterised previously in several NMR studies [40–42]: conformation I has its positively charged nicotinamide ring bound within the enzyme (the 'in' conformation); and conformation II has the positive nicotinamide ring extending away from the enzyme surface into solution (the 'out' conformation). In the present work, only the chemical shifts corresponding to the 'in' conformation are relevant.

Tables 1 and 2 present the ^{1}H and ^{15}N chemical shifts of nuclei for some of the DHFR residues (Ala

Table 1
^{15}N chemical shifts (Chemical shifts referenced to liquid NH_3) (in ppm) of NH groups for some residues in the nicotinamide site

Residue	Inhibitor	Complex with NADPH			Complex with $NADP^+$		
		δ Ternary	δ Binary[a]	Δδ (T–B)	δ Ternary	δ Binary[a]	Δδ (T–B)
Ala 6	TMP	124.70	122.00	+ 2.70	121.35	122.00	− 0.65
	MTX	124.00	121.70	+ 2.30	121.20	121.70	− 0.50
	TMQ	–	–	–	121.70	122.20	− 0.50
Gln 7	TMP	114.30	114.60	− 0.30	117.67	114.60	+ 3.07
	MTX	114.00	114.75	− 0.75	117.40	114.75	+ 2.65
	TMQ	–	–	–	117.40	114.80	+ 2.60
Ile 13	TMP	112.10	112.10	0.00	109.50	112.10	− 2.60
	MTX	111.60	112.10	− 0.50	109.40	112.10	− 2.70
	TMQ	–	–	–	109.50	112.40	− 2.90
Gly 14	TMP	105.90	106.10	− 0.20	111.34	106.10	+ 5.24
	MTX	105.40	106.50	− 1.10	110.80	106.50	+ 4.30
	TMQ	–	–	–	111.00	107.10	+ 3.90

[a] The binary complexes are complexes of DHFR with TMP, MTX or TMQ in the absence of coenzyme.

6, Gln 7, Ile 13 and Gly 14) in the binding site of the reduced or oxidised nicotinamide ring in the different binary and ternary complexes containing the coenzymes. In order to evaluate the effect of the bound coenzyme on the DHFR ^1H and ^{15}N chemical shifts the ligand-induced chemical shift differences (LCSs) for NADPH and $NADP^+$ were calculated and analysed. Positive LCSs values indicate a deshielding induced by the binding of ligand (coenzyme) relative to the corresponding ligand-free (coenzyme-free) protein.

The data presented in Tables 1 and 2 indicate that there are significant changes in the electronic states of residues surrounding the nicotinamide moiety upon replacing NADPH by $NADP^+$. It is apparent that the LCSs for NADPH and $NADP^+$ are not equivalent. For example, the ^{15}N for the NH group of Gln 7 is around $+2.7$ ppm for $NADP^+$, while it is around -0.5 ppm for NADPH. The effect of binding NADPH or $NADP^+$ has opposite shielding effects on the nuclei of the residues shown in Tables 1 and 2 suggesting that the oxidation state of the cofactors

Table 2
^1H chemical shift (Chemical shifts referenced to DSS (sodium 2,2-dimethyl-2-silapentane-5-sulfonate) (in ppm) of NH groups for some residues in the nicotinamide site

Residue	Inhibitor	Complex with NADPH			Complex with $NADP^+$		
		δ Ternary	δ Binary[a]	Δδ (T–B)	δ Ternary	δ Binary[a]	Δδ (T–B)
Ala 6	TMP	10.75	8.62	+ 2.13	9.07	8.62	+ 0.45
	MTX	10.29	8.57	+ 1.72	8.93	8.57	+ 0.36
	TMQ	–	–	–	9.13	8.59	+ 0.54
Gln 7	TMP	9.17	9.03	+ 0.14	9.43	9.03	+ 0.40
	MTX	9.05	8.97	+ 0.08	9.36	8.97	+ 0.39
	TMQ	–	–	–	9.40	9.06	+ 0.34
Ile 13	TMP	9.04	8.97	+ 0.07	9.32	8.97	+ 0.35
	MTX	8.94	8.95	− 0.01	9.27	8.95	+ 0.32
	TMQ	–	–	–	9.20	8.93	+ 0.27
Gly 14	TMP	7.76	7.49	+ 0.27	8.08	7.49	+ 0.59
	MTX	7.66	7.49	+ 0.17	8.06	7.49	+ 0.57
	TMQ	–	–	–	8.04	7.52	+ 0.52

[a] The binary complexes are complexes of DHFR with TMP, MTX or TMQ in the absence of coenzyme.

Table 3
Charges on C=O and N–H atoms for the nicotinamide amide group, and for the protein amide groups CO(Trp 5)–NH(Ala 6) and CO(Ala 6)–NH(Gln 7) calculated for System 1

	NADPH	$NADP^+$	Δ(NADPH–$NADP^+$)
Nicotinamide(O)	− 0.55859	− 0.49048	− 0.0681
Nicotinamide(N)	− 0.56536	− 0.61007	+ 0.0447
Nicotinamide(HN)	0.38189	0.511502	− 0.1296
Trp 5(O)	− 0.52613	− 0.49134	− 0.0348
Ala 6(N)	− 0.26506	− 0.23687	− 0.0282
Ala 6(HN)	0.427438	0.345543	+ 0.0819
Ala 6(O)	− 0.57206	− 0.63214	+ 0.0601
Gln 7(N)	− 0.21886	− 0.20813	− 0.0107

play a central role in modifying the electronic environment of these nuclei. Thus, even though the pattern of hydrogen bonding is qualitatively similar (same donor and acceptor) quite different shielding is observed. Only relatively small deshielding contributions are expected from ring current effects. A ^1H deshielding contribution of 0.17 ppm is estimated from ring current calculations [44] for the Ala 6 NH proton due to the aromatic nicotinamide ring of $NADP^+$. For residues Gln 7, Ile 13 and Gly 14 the ring current deshielding is estimated to be less than 0.03 ppm. These deshielding contributions will have only a small effect on the chemical shift differences between the NADPH and $NADP^+$ complexes.

Some of the chemical shift changes observed upon binding to NADPH or $NADP^+$ can be easily rationalised. The nicotinamide H_2N forms hydrogen bonds with the carbonyl oxygen atom of residues Ala 6 and Ile 13 (Fig. 1) and, for $NADP^+$, the nicotinamide ring positive charge delocalised onto the H_2N protons (see Table 3) would be expected to cause a deshielding of the ^{15}N nuclei in the NH groups directly attached to these carbonyls (Gln 7 and Gly 14) due to the stabilisation of the polarised form of the amide [45,46]. A large deshielding of these ^{15}N nuclei is observed for the $NADP^+$ complexes (around +3.0 ppm for Gln 7 and +4.5 ppm for Gly 14 as shown in Table 1). However, for the NADPH complexes this effect is much smaller (namely around −0.5 ppm for Gln 7 and around −0.5 ppm for Gly 14).

3.3. DFT geometry optimisation calculations of nicotinamide-coenzyme interactions

In order to obtain insights into the factors controlling the trends in the measured ^1H and ^{15}N chemical shift reported in Tables 1 and 2 for the DHFR complexes with the reduced and oxidised form of the coenzyme, DFT calculations [47] using GAUSSIAN

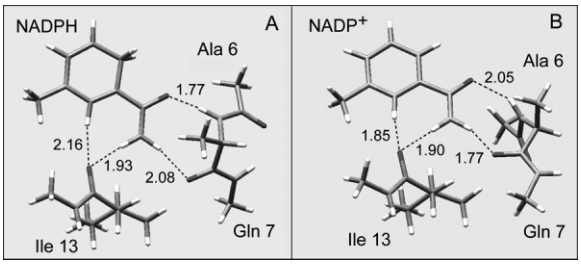

Fig. 3. DFT optimised geometry of model System 1 showing the interactions of protein backbone atoms of residues Ala 6, Gln 7 and Ile 13 with (A) the reduced nicotinamide ring (B) the oxidised nicotinamide ring of the coenzyme. Hydrogen atoms are coloured white and oxygen atoms dark grey. The hydrogen bonds are indicated with dotted lines, and the hydrogen bond distances (in Å) for A and B are shown in the figure.

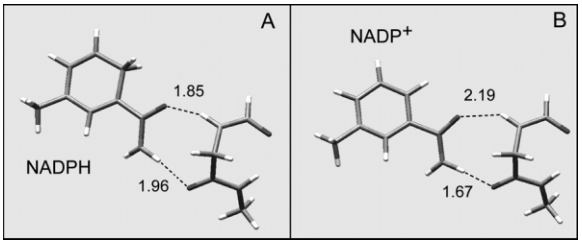

Fig. 4. DFT optimised geometry of model System 2 showing the interactions of protein backbone atoms of residues Ala 6 and Gln 7 with (A) the reduced nicotinamide ring (B) the oxidised nicotinamide ring of the coenzyme. Hydrogen atoms are coloured white and oxygen atoms dark grey. The hydrogen bonds are indicated with dotted lines, and the hydrogen bond distances (in Å) for A and B are shown in the figure.

Table 4
Calculated and experimental chemical shifts of ^{1}H and ^{15}N nuclei in nicotinamide fragment and interacting amino acid residues of DHFR. Calculation was performed on System 1. NMR chemical shifts were calculated using GIAO method with B3LYP 6.311++(2d,p) basis set

Atom	Calculated			Experimental
	NADPH	$NADP^+$	Difference	Difference
^{15}N (HN Ala 6)	127.75	120.26	7.49	3.20
^{1}H (HN Ala 6)	9.71	6.94	2.77	1.60
^{15}N (HN Gln 7)	113.17	121.82	− 8.65	− 3.10
^{1}H (HN Gln 7)	7.19	7.52	− 0.33	− 0.16
^{1}H (HN coenzyme)	7.62	13.00	− 5.38	− 2.87

[28] were carried out. The initial coordinates for the GAUSSIAN calculations were obtained from the NMR determined solution structure of the DHFR–NADPH–TMP complex [16] and included the nicotinamide moiety and some of the relevant DHFR residues in the coenzyme binding site. Two sets of molecular fragments were used as models for subsequent calculations. The larger set is shown in Fig. 3 (System 1) and includes the nicotinamide fragment of the coenzyme and protein residues involved in H-bond interactions (backbone of residues Ala 6, Ile 13, Gln 7 and Gly 14). The second smaller set is shown in Fig. 4 (System 2) and includes the coenzyme nicotinamide fragment interacting with the shorter stretch of protein backbone (residues Ala 6 and Gln 7). This set was used to investigate in more detail the influence of the oxidation state of the nicotinamide ring on the strength and geometry of the pairs of H-bonds, formed by donor (NH) and acceptor (CO) simultaneously.

Geometry optimisation of the System 1 model was carried out using the Hartree–Fock method (with 3-21G basis set). All atoms, including those belonging to the protein, were allowed to move during the geometry optimisation calculations. It was found that H-bond interactions changed significantly upon changing the oxidation state of nicotinamide ring. In the case of NADPH, the shortest H-bond was between the oxygen atom of the coenzyme carboxamide group and the HN proton of Ala 6. For NADPH the H-bonds involving donors from the coenzyme part were much weaker than for $NADP^+$ (Fig. 3). When NADPH was replaced by $NADP^+$, the strongest hydrogen bonds were formed between protons of the coenzyme and acceptors in the protein residues (the oxygen atoms of backbone CO groups of Ala 6 and Ile 13). Thus, with replacement of NADPH by $NADP^+$, the distance $d(O_{nicotinamide}–HN_{Ala6})$ increased from 1.77 to 2.05 Å, whereas the distance $d(O_{Ala6}–H_2N_{nicotinamide})$ decreased from 2.08 to 1.77 Å. To accommodate such a change it would be necessary for the orientation of the nicotinamide ring relative to the β-strand A of DHFR to be different in the two complexes.

The interactions with Ala 6 and Gln 7 were examined in detail by using the more precise DFT methods (B3LYP with 6.311G 3d, 2p basis set) on the second smaller set of atoms involving only Ala 6 and Gln 7 as the interacting protein residues (System 2). In this case the geometries of the protein residues were kept fixed but the atoms of the nicotin amide moiety were allowed to move. The results obtained from these calculations were similar to those described above (see Fig. 4). Upon changing NADPH for $NADP^+$, the distance $d(O_{nicotinamide}–HN_{Ala6})$ increased from 1.85 to 2.19 Å, and the distance $d(O_{Ala6}–H_2N_{nicotinamide})$ decreased from 1.96 to 1.67 Å. ^{1}H chemical shifts of NH protons are known to be very sensitive to changes in hydrogen bond lengths [47,48].

3.4. Calculated charges in model systems in NADPH and $NADP^+$

Table 3 presents the calculated charges on the oxygen and nitrogen atoms in the nicotinamide carboxamide group, and in the protein amide groups CO(Trp 5) –NH(Ala 6) and CO(Ala 6)–H(Gln 7). It can be seen that the oxygen atom of the nicotinamide carboxamide group in the NADPH system is more negatively charged than in the $NADP^+$, and hence should be a better H-bond acceptor than in $NADP^+$. Consistently, the Ala 6 NH proton hydrogen bonded

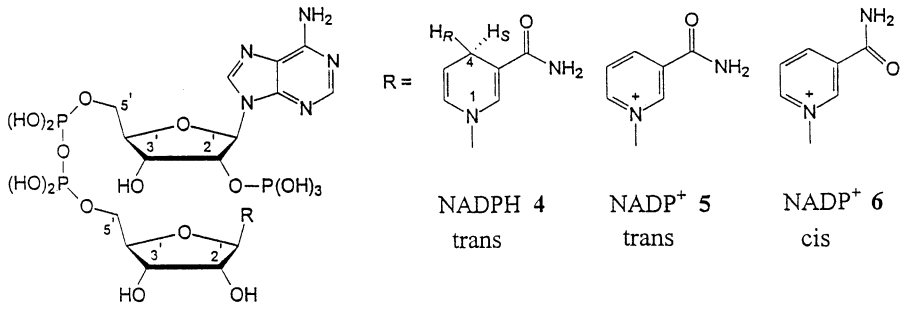

Scheme 2.

to this oxygen atom is 0.0819 units more positive in NADPH than in $NADP^+$ indicating that in NADPH the hydrogen bond would be expected to be stronger than in $NADP^+$.

In addition, it can be seen from Table 3 that the nicotinamide carboxamide group NH proton that is H-bonded to the CO of Ala-6, is more positive by 0.1296 units in $NADP^+$ than in NADPH, and similarly the CO oxygen atom of Ala 6 is more negative by 0.0601 units. Hence, the hydrogen bond between nicotinamide carboxamide NH_2 to the CO of Ala 6 is stronger for $NADP^+$ than for NADPH.

3.5. GIAO calculations of ^1H and ^{15}N chemical shieldings in model fragments

In order to obtain insights into the factors defining the ^1H and ^{15}N chemical shift trends observed in Tables 1 and 2, GIAO calculations were performed on System 2. In Table 4 the GIAO calculated chemical shielding differences are compared with the experimental values. It was found that the calculated $\delta(^{15}N)$ chemical shift difference between the NADPH and $NADP^+$ systems for the amide nitrogen of Ala 6 was -7 ppm, whereas that of Gln 7 was $+8$ ppm (Table 4). This is in good qualitative agreement with the experimental results (-3.2 and $+3.3$ ppm, respectively). The absolute values of the calculated chemical shift differences are bigger in magnitude than the experimental values and this could arise because the calculations take no account of the environmental effects of neighbouring residues and solvent, nor for any deviations from optimal hydrogen bonding geometries (see later). Most importantly, the relative changes in ^{15}N chemical shifts of Ala 6 and Gln 7 are in good agreement with the experimental trends, thus confirming the validity of the calculated results.

3.6. Difference in binding affinities of NADPH and $NADP^+$

Several workers have applied *ab initio* calculations to reduced and oxidised nicotinamide ring fragments in vacuo and in solution in order to predict charge distributions, energies and conformations [13,14]. The calculations predicted that the oxidised nicotinamide ring amide group would be predominantly in the *cis*-conformation whereas that of the reduced form would be in the *trans*-conformation in solution [13,14]. The *trans*- and *cis*-conformations refer to the relative orientations of the carboxamide oxygen atom and N1 as shown in structures **5** and **6** in Scheme 2 (structures **4**–**6** (NADPH and $NADP^+$ (*trans*- and *cis*-conformations)). The energy difference between the *cis*- and *trans*-forms of $NADP^+$ in solution was calculated to be 12.0 kJ/mol [14]. The results of the energy calculations agree with the experimental X-ray data for oxidised nicotinamide rings that show the preferred conformation in the crystal to be the *cis*-conformation [13]. However, X-ray [15] and NMR [16] structural studies of the coenzymes bound to DHFR show that the carboxamide group is in the *trans*-conformation for both NADPH and $NADP^+$ in the bound state. Thus, $NADP^+$ needs to change from a mainly *cis*-conformation in solution to a *trans*-conformation on binding to DHFR and therefore requires energy for this conformational change (calculated as 12.0 kJ/mol [14]). Since only $NADP^+$ in its *trans*-conformation binds to DHFR, this *cis*/*trans* energy

difference of 12.0 kJ/mol causes an effective ~100 fold reduction in the binding affinity of $NADP^+$. In contrast, if NADPH is predominantly in a *trans*-conformation in solution, as indicated by the calculations [14], it would have a smaller *cis*/*trans* energy penalty upon binding to DHFR. It should be mentioned that earlier Raman studies suggested that free NADPH in solution has a substantial amount of the *cis*-conformation that converts to the *trans*-form on binding to *E. coli* dihydrofolate reductase [8].

In model System 2, in order to estimate the total interaction energy between the nicotinamide ring of the coenzyme and the interacting protein residues for both NADPH and $NADP^+$, energy calculations were carried out for the whole system and for the individual interacting fragments. The total interaction energy was taken as the difference in energy between that of the whole system (the interacting protein residues and the nicotinamide ring of the coenzyme) and the sum of the energies of the isolated components (the interacting protein residues alone, and the nicotinamide ring of the coenzyme alone). The calculated interaction energies are −63.05 kJ/mol for the NADPH system and −72.34 kJ/mol for the $NADP^+$ system. Thus, if the reduced and oxidised rings of the bound coenzymes could each take up their optimal hydrogen bonding geometries, then $NADP^+$ would in fact bind tighter than NADPH. However, it appears that $NADP^+$ cannot take up its optimal hydrogen bond geometry as discussed below.

If the protein backbones of the model System 2 (see Fig. 4) calculated with reduced and oxidised forms of nicotinamide are superimposed, the nicotinamide rings of the two coenzymes remain in the same plane but their N_1–C_4 axis differ in orientation by 15°. According to the crystallographic data the reduced and oxidised nicotinamide rings occupy the same binding site in NADPH and $NADP^+$ complexes with DHFR [15,16]. Because Ala 6 and Gln 7 form part of a β-sheet in a conformationally rigid part of the protein then, in order for the oxidised and reduced nicotinamide rings to occupy the same site, at least one of the two coenzymes cannot be taking up its optimised H-bond geometry. If it is assumed that the tighter binding NADPH binds to DHFR with an optimised hydrogen bonding pattern and that it is the bound $NADP^+$ nicotinamide ring that does not adopt its optimal H-bond geometry, this could result in a considerable loss of binding energy. The 1500 fold decrease observed in binding affinity of $NADP^+$ compared to NADPH corresponds to an energy difference of ~18 kJ/mol. Even allowing for the 12.0 kJ/mol contribution which would be lost by the oxidised nicotinamide carboxamide group having to change from a *cis*- to a *trans*-conformation on binding to the enzyme [14] there is still a 6 kJ/mol loss in binding energy that requires explanation. Some idea of the potential loss of energy resulting from incorrect geometry of the $NADP^+$ can be obtained by calculating the energy difference upon changing the nicotinamide ring from the reduced to the oxidised form for System 2 with both rings superimposed on the position of the reduced nicotinamide ring. The energy of the oxidised nicotinamide ring in this conformation is higher than that in its optimal conformation by ~80 kJ/mol. Thus the 18 kJ/mol difference observed experimentally could easily result from the 12 kJ/mol required for the *cis*/*trans* rotation and a further 6 kJ/mol contribution from the nicotinamide ring of $NADP^+$ being unable to take up its optimal conformation to achieve the ideal H-bond geometries of the interactions between the nicotinamide ring amide group and the backbone of residues Ala 6 and Gln 7. The rigidity of these residues could prevent the changes in the geometry of the interaction between the protein and the oxidised nicotinamide ring required to reach its optimal binding potential.

3.7. Comparison with other enzymes that use NADPH as a cofactor

Analyses of available three-dimensional structures of NADPH-dependent enzymes other than DHFR (using data from Brookhaven Protein Data Bank) showed that hydrogen bond interactions of the nicotinamide amide group with protein residues usually have a geometry of interaction similar to that found in DHFR-coenzyme complexes. In almost all cases analysed the interactions involve protein backbone atoms (CO oxygen atoms and HN protons) deeply buried inside the protein. The interacting part of the protein is usually situated inside the protein, where the relevant stretch of protein backbone is unlikely to be flexible enough to easily accommodate changes in geometry of H-bonds upon oxidising the nicotinamide ring.

4. Concluding remarks

The quantum mechanical calculations used in this study are clearly useful for predicting energies and hydrogen bond lengths in interacting systems. The calculated differences between corresponding H-bonds in NADPH and $NADP^+$ systems are within 0.3 Å. It is unlikely that precision of this order can be achieved in typical X-ray and NMR structure determinations. Moreover, because X-ray does not detect hydrogens the observed precision in estimates of H-bond distances will be even smaller. The values of NMR shielding constants calculated using quantum mechanical methods compare well with experimental data and hence provide a useful tool for studying subtle changes in geometry of protein-ligand interactions. Such small changes in fine structure could play an important role in biochemical processes. The NMR measurements were carried out at the MRC Biomolecular NMR Centre, Mill Hill.

Acknowledgements

This work was supported by the Medical Research Council and by a Wellcome Trust Collaborative Research Initiative Grant 060140. VIP acknowledges the award of a Howard Hughes Medical Institute International Scholarship and a grant from the Russian Foundation for Basic Research (99-04-48288). Dr P.M. Nieto is thanked for assistance with the assignments of the DHFR–NADPH–MTX complex and for useful discussions.

References

[1] R.L. Blakley, Dihydrofolate reductase, in: R.L. Blakley, S.J. Benkovic (Eds.), Folates and Pterins, vol. 1, Wiley, New York, 1985, pp. 191–253 Chapter 5.
[2] Y.D. Wu, K.N. Houk, J. Org. Chem. 58 (1993) 2043.
[3] B. Birdsall, A.S.V. Burgen, G.C.K Roberts, Biochemistry 19 (1980) 3723.
[4] B. Birdsall, A.S.V. Burgen, G.C.K. Roberts, Biochemistry 19 (1980) 3732.
[5] C.A. Fierke, K.A. Johnson, S.J. Benkovic, Biochemistry 26 (1987) 4085.
[6] J. Andrews, C.A. Fierke, B. Birdsall, G. Ostler, J. Feeney, G.C.K. Roberts, S.J. Benkovic, Biochemistry 28 (1989) 5743.
[7] P.L. Cummings, J.E. Gready, THEOCHEM-J. Mol. Struct. 52 (1989) 161.
[8] J. Zheng, Y.Q. Chen, R. Callender, Eur. J. Biochem, 215 (1993) 9.
[9] Y.D. Wu, D.K.W. Lai, K.N. Houk, J. Am. Chem. Soc. 117 (1995) 4100.
[10] R.A. Torres, B. Schiott, T.C. Bruice, J. Am. Chem. Soc. 121 (1999) 8164.
[11] S.P. Greatbanks, J.E. Gready, A.C. Limaye, A.P. Rendell, J. Comput. Chem. 21 (2000) 788.
[12] Q. Cui, M. Karplus, J. Phys. Chem. B104 (2000) 3721.
[13] H. Li, B.M. Goldstein, J. Med. Chem. 35 (1992) 3560.
[14] G.D. Luca, T. Marino, T. Mineva, N. Russo, M. Toscano, THEOCHEM-J. Mol. Struct. 501–502 (2000) 215.
[15] M.R. Sawaya, J. Kraut, Biochemistry 36 (1997) 586.
[16] V.I. Polshakov, B. Birdsall, J. Feeney, Unpublished results.
[17] C. Bystroff, S.J. Oakley, J. Kraut, Biochemistry 29 (1990) 3263.
[18] S.J. Hammond, B. Birdsall, M.S. Searle, G.C.K. Roberts, J. Feeney, J. Mol. Biol. 188 (1986) 81.
[19] J.G. Dann, G. Ostler, R.A. Bjur, R.W. King, P. Scudder, P.C. Turner, G.C.K. Roberts, A.S.V. Burgen, N.G.L. Harding, Biochem. J. 157 (1975) 559.
[20] J. Andrews, G.M. Clore, R.W. Davies, A.M. Gronenborn, B. Gronenborn, D. Kalderon, P.C. Papadopoulos, S. Schafer, P.F.G. Sims, R. Stancombe, Gene 35 (1985) 217.
[21] V. Sklenar, M. Piotto, R. Leppik, V. Saudek, J. Magn. Reson., Ser. A 102 (1993) 241.
[22] A.J. Shaka, P.B. Barker, R. Freeman, J. Magn. Reson. 64 (1985) 547.
[23] D.J. States, R.A. Haberkorn, D.J. Ruben, J. Magn. Reson. 48 (1982) 286.
[24] S. Mori, Abeygunawardana, M. O'Neil Johnson, P.C.M. Van Zijl, J. Magn. Reson., Ser. B 108 (1995) 94.
[25] B. Birdsall, V.I. Polshakov, J. Feeney, Biochemistry 39 (2000) 9819.
[26] V.I. Polshakov, B. Birdsall, T.A. Frenkiel, A.R. Gargaro, J. Feeney, Protein Sci. 8 (1999) 1.
[27] M.D. Carr, B. Birdsall, T.A. Frenkiel, C.J. Bauer, J. Jimenez-Barbero, V.I. Polhakov, J.E. McCormick, G.C.K. Roberts, J. Feeney, Biochemistry 30 (1991) 6330.
[28] M.J. Frisch, G.W. Trucks, H.B. Schlegel, G.E. Scuseria, M.A. Robb, J.R. Cheeseman, V.G. Zakrzewski, J.A. Montgomery, R.E. Stratmann, J.C. Burant, S. Dapprich, J.M. Millam, A.D. Daniels, K.N. Kudin, M.C. Strain, O. Farkas, J. Tomasi, V. Barone, M. Cossi, R. Cammi, B. Mennucci, C. Pomelli, C. Adamo, S. Clifford, J. Ochterski, G.A. Petersson, P.Y. Ayala, Q. Cui, K. Morokuma, D.K. Malick, A.D. Rabuck, K. Raghavachari, J.B. Foresman, J. Cioslowski, J.V. Ortiz, B.B. Stefanov, G. Liu, A. Liashenko, P. Piskorz, I. Komaromi, R. Gomperts, R.L. Martin, D.J. Fox, T. Keith, M.A. Al-Laham, C.Y. Peng, A. Nanayakkara, C. Gonzalez, M. Challacombe, P.M.W. Gill, B.G. Johnson, W. Chen, M.W. Wong, J.L. Andres, M. Head-Gordon, E.S. Replogle, J.A. Pople, GAUSSIAN 98, Gaussian, Inc., Pittsburgh PA, 1998.
[29] J.S. Binkley, J.A. Pople, W.J. Hehre, J. Am. Chem. Soc. 102 (1980) 932.

[30] M.S. Gordon, J.S. Binkley, J.A. Pople, W.J. Pietro, W.J. Hehre, J. Am. Chem. Soc. 104 (1982) 2797.
[31] W.J. Pietro, M.M. Francl, W.J. Hehre, D.J. Deffrees, J.A. Pople, J.S. Binkley, J. Am. Chem. Soc. 104 (1982) 5039.
[32] R.G. Parr, W. Yang, Density Functional Theory of Atoms and Molecules, Oxford University Press, Oxford, 1989.
[33] A.D. McLean, G.S. Chandler, J. Chem. Phys. 72 (1980) 5639.
[34] R. Krishnan, J.S. Binkley, R. Seeger, J.A. Pople, J. Chem. Phys. 72 (1980) 650.
[35] A.D. Becke, J. Chem. Phys. 98 (1988) 785.
[36] C.T. Lee, W.T. Yang, R.G. Parr, Phys. Rev. B 37 (1988) 785.
[37] C. Peng, P.Y. Ayala, H.B. Schlegel, M..J. Frisch, J. Comput. Chem. 17 (1996) 49.
[38] K. Wolinski, J.F. Hinton, P. Pulay, J. Am. Chem. Soc. 112 (1990) 8251.
[39] G.L. Martin, M.L. Martin, J.-P. Gouesnard, 15N-NMR spectroscopy, in: P. Diehl, E. Fluck, R. Kostfeld (Eds.), NMR Basic Principles and Progress, vol. 50, Springer, Berlin, 1981.
[40] A. Gronenborn, B. Birdsall, E.I. Hyde, G.C.K. Roberts, J. Feeney, A.S.V. Burgen, Mol. Pharmacol. 20 (1981) 145.
[41] B. Birdsall, A.W. Bevan, C. Pascual, G.C.K. Roberts, J. Feeney, A. Gronenborn, G.M. Clore, Biochemistry 23 (1984) 4733.
[42] V.I. Polshakov, B. Birdsall, J. Feeney, Biochemistry 38 (1999) 15,962.
[43] A.R. Gargaro, A. Soteriou, T.A. Frenkiel, C.J. Bauer, B. Birdsall, V.I. Polshakov, I.L. Barsukov, G.C.K. Roberts, J. Feeney, J. Mol. Biol. 277 (1998) 119.
[44] C.E. Johnson, F.A. Bovey, J. Chem. Phys. 29 (1958) 1012.
[45] A.C. De Dios, J.G. Pearson, E. Oldfield, Science 260 (1993) 1491.
[46] R.R. Biekofsky, S.R. Martin, J.P. Browne, P.M. Bayley, J. Feeney, Biochemistry 37 (1998) 7617.
[47] U. Sternberg, E. Brunner, J. Magn. Reson., Ser. A 108 (1994) 142.
[48] W.D. Morgan, B. Birdsall, P.M. Nieto, A.R. Gargaro, J. Feeney, Biochemistry 38 (1999) 2127.